Shear-Compression Test on Masonry Walls with an Innovative Experimental Setup

Published Version:
Ferretti, F., Pozza, L., Mazzotti, C. (2023). Shear-Compression Test on Masonry Walls with an Innovative Experimental Setup [10.1007/978-3-031-39603-8_42].

Availability:
This version is available at: https://hdl.handle.net/11585/961380 since: 2024-02-25

Published:

DOI: http://doi.org/10.1007/978-3-031-39603-8_42

Shear-Compression Test on Masonry Walls with an Innovative Experimental Setup

Francesca Ferretti[1][0000-0003-1484-3853], Luca Pozza[1][0000-0001-7087-8386] and Claudio Mazzotti[1][0000-0002-5314-4687]

[1] University of Bologna, DICAM Department, Viale Risorgimento 2 - 40136 Bologna, Italy
`francesca.ferretti10@unibo.it`

Abstract. The behavior and failure mechanism of a masonry wall subject to in-plane shear depends on several factors, such as the wall geometry, the boundary conditions, the acting stresses, and the masonry mechanical parameters. The objective of this research was the study of the in-plane shear behavior of full-scale masonry panels through an innovative experimental setup, purposely designed to reproduce a double fixed boundary condition in order to induce a diagonal cracking failure mode. Such a boundary condition was ensured by the presence of an upper horizontal rigid steel beam, combined with the possibility of modulating the compressive load applied to the masonry panel, while increasing the horizontal displacement. Nonlinear numerical simulations were carried out to analyze the capability of the experimental setup of reproducing the desired loading and restraint conditions and to predict the shear behavior of a clay brick masonry panel. A finite element model was realized, in which all the components of the experimental setup were included to account for all possible failure modes, and the masonry panel was modelled according to a macro-modelling approach. The results of the numerical predictions were compared with the results of a shear-compression test on a masonry panel, which will be presented in the paper. The good agreement obtained between the numerical and the experimental results, both in terms of load *vs* displacement curve and development of the cracking process, confirmed the suitability of the setup in reproducing the assumed boundary conditions and shear failure mode.

Keywords: Masonry, In-plane Behavior, Shear-compression Test, Experimental Setup, Numerical Prediction.

1 Introduction

A masonry pier subject to shear can fail according to a rocking, sliding or diagonal cracking failure mode, depending on the element geometry, the acting tangential and normal stresses, the boundary conditions, and the masonry mechanical parameters [1–3]. With reference to the typical boundary conditions of a masonry pier in an existing masonry building, the following limit conditions can be considered: (i) clamped base and free rotation at the top (cantilever boundary condition); (ii) doubly clamped condition with restrained rotation at the top (double fixed boundary condition). Factors mainly affecting the occurrence of one of the cited conditions, or an intermediate condition between the two, are: the slab typology, the quality of the connections between the structural elements, the presence of reinforced concrete curbs or ring beams, and the presence of strong or weak spandrels. In this research, a particular focus will be devoted to the double fixed boundary condition, which can be encountered, in the engineering practice, in existing buildings characterized by the presence of RC curbs, guaranteeing a good connection between horizontal and vertical structural elements providing a box-like behavior, and of spandrels able to provide an adequate coupling between the masonry piers [4,5].

With the objective of studying the shear behavior of masonry, several experimental setups were proposed in the literature for the execution of in-plane shear tests on masonry panels [6,7]. The variability of these setups was mainly related to the boundary conditions, the presence of a vertical load, and the way of application of the horizontal load to the samples, highlighting the need to correctly design such systems to reproduce the desired shear failure. More specifically, the horizontal force was usually applied to the masonry panel by means of a rigid steel beam, aimed at redistributing the shear force over the entire cross section of the sample. In addition, a vertical compressive stress was applied to the masonry panel to reduce the tensile stresses at the base of the masonry panel and, in some cases, a proper restraint was introduced to prevent the rotation of the top cross section of the masonry panel, given by the application of the horizontal force. In this way, it was possible to achieve the desired stress condition within the sample, and to obtain the correspondent failure mode [8-10]. The differences observed between the adopted test setups highlight the need to focus on the proper design of such systems and on the use of appropriate testing procedures to reproduce the desired shear behavior.

In the following, the design of an innovative experimental setup for the execution of in-plane shear tests on masonry panels is presented, together with the numerical prediction and the experimental validation. The experimental setup aims at reproducing a double fixed boundary condition. The elements characterizing its novelty are the possibility to modulate the vertical load during the tests to reduce the rotation of the top cross section, the presence of a horizontal rigid steel beam supported by rollers, providing a further constraint to the rotation, and the application of the shear load in correspondence with the centerline of the masonry panel.

2 Innovative Experimental Setup

2.1 Description of the Experimental Setup

The innovative experimental setup was designed with the aim of conducting monotonic and cyclic coupled compression-shear tests on full-scale masonry panels with a double fixed boundary condition to induce a diagonal cracking failure. The maintenance of such boundary condition during the test is ensured by the special conformation of the setup, i.e., the presence of an upper horizontal rigid steel beam, combined with the modulation of the applied compressive load (N). In more detail, the variation of the point of application of the compressive load as the imposed horizontal displacement (i.e. the shear load) increases allows to limit the rotation of the top cross section of the masonry panel and to reproduce as closely as possible the desired boundary condition.

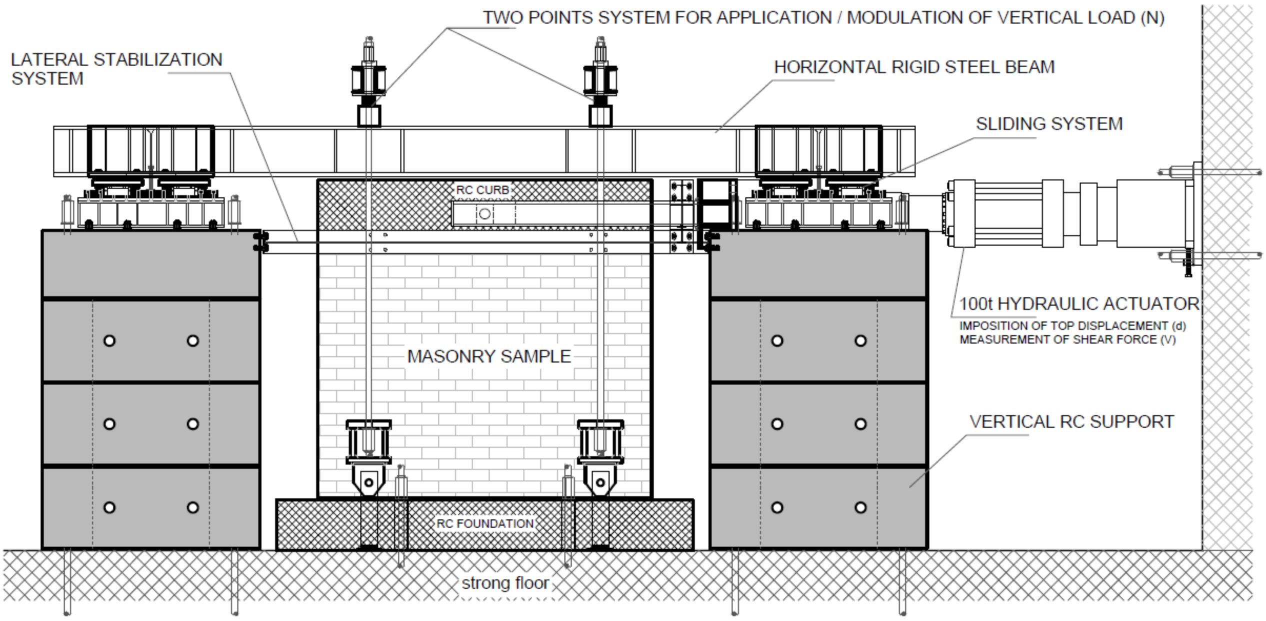

Fig. 1. Scheme of the experimental setup.

The scheme of the experimental setup is reported in Fig. 1 and it is composed by the following key elements:

- Vertical RC supports for the fastening of the sliding system: positioned on the sides of the testing sample, they are realized with RC hollow elements, connected together and properly fixed to the laboratory strong floor. They constitute the support system for the horizontal rigid steel beam and for the sliding system (i.e. rollers).
- Horizontal rigid steel beam: composed by a HEB 300 steel profile and installed on rollers, it represents the constraint for the top cross section of the masonry sample. The horizontal beam is equipped with four cantilever elements, positioned at the extremities, for the connection with the sliding system, fixed to the vertical RC supports. The beam acts as a rigid element also to provide an adequate redistribution of the vertical compressive load.
- System for the application of the horizontal displacement: it is composed by a horizontal hydraulic actuator (capacity of 1000 kN), fixed to a rigid contrast wall. The horizontal displacement is applied at the top of the testing sample by means of a forked steel element, fixed rigidly, on one side, to the hydraulic actuator and, on the other side, to the centroid of the top RC curb through a thick steel pin. Local damages due to the pin-concrete contact are avoided by the presence of a steel element casted within the RC curb to redistribute the stresses. Connections between the steel elements are realized by precision machining to reduce backlash.
- Two-point system for the imposition and modulation of the vertical load: the vertical load is applied to the masonry panel by means of a closed system, in which two hydraulic jacks, having a capacity of 500 kN, are interposed between the horizontal rigid steel beam and rigid steel elements connected to the foundation through DYWIDAG bars. This system, composed by vertical rods, allows to maintain the compressive load constant within the expected range of horizontal displacements during the test. The modulation of the compressive load is carried out by varying the pressure

of each hydraulic jack, that is by increasing the pressure in one jack and decreasing it in the other jack, depending on the versus of applied horizontal displacement.
- Lateral stabilization system: it is constituted by two HEB 140 steel profiles, fixed rigidly to the vertical RC supports. The profiles are equipped with rollers in contact with the testing sample preventing out-of-plane displacements while allowing the horizontal sliding of the sample.
- Test sample: it is composed by the masonry panel, an upper RC curb and a base RC foundation. The RC foundation is fixed to the strong floor with post-tensioned DYWIDAG bars, and it is equipped with four steel plates which allow the connection of the vertical rods used for the application of the compressive load. The masonry panel has dimensions of 2000×1500×250 mm^3 and it is built over the RC foundation. The top RC curb, casted over the masonry panel, allows the diffusion of both the vertical load and the application of the horizontal displacement to the masonry panel.

2.2 Testing Procedure

The testing procedure involves three consequential phases (Fig. 2). In Phase 1, the vertical load (N) is symmetrically applied to the masonry panel. In this phase, the rigid steel beam is not connected to the sliding system and, therefore, to the vertical RC supports in order to avoid load migration from the masonry panel to the vertical RC supports. In Phase 2, the sliding system is activated. During Phase 3, the horizontal displacement is applied.

For small displacement level, the rotation of the top section of the masonry panel (and therefore the detachment of the sample from the steel beam) is counteracted by the rigid steel beam, while for high displacement level, it is also necessary to modulate the vertical load (N) by progressively increasing the vertical force acting on the side of the wall panel which tends to uplift and by reducing the one on the opposite side, maintaining constant, at each step, the global vertical load (N). Clearly, the maximum applicable variation of the vertical loads implies the maximization of the load, i.e., load equal to the global one, on the side which tends to uplift, and the minimization of the load, i.e. null load, on the other side. The modulation of the vertical load in function of the imposed horizontal displacement (load) level can be performed according to specific laws, e.g., the ones used for the numerical prediction and experimental validation presented in the following.

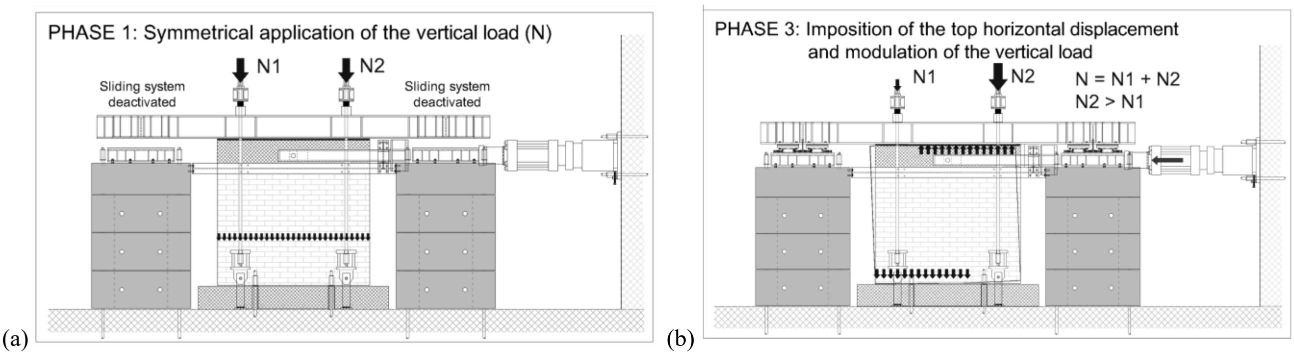

Fig. 2. Testing procedure: (a) Phase 1, (b) Phase 3.

3 Numerical Prediction and Experimental Validation

In this section, the capability of the experimental setup of reproducing the desired boundary conditions and the diagonal shear failure of the masonry panel is studied from both the numerical and experimental point of view. In more detail, the first cyclic shear-compression test was performed, and a numerical prediction was conducted in which a Finite Element model of the experimental setup was realized, including most of the key elements described in Section 2.

Conditions under which both the numerical analysis and experimental tests were performed are the same, in terms of vertical stress applied, horizontal displacement imposed in each loading cycle, modulation of the vertical load during the test, and material properties. Specifically, the vertical stress applied was equal to 0.4 MPa. In Fig. 3, the cyclic loading imposed in terms of horizontal displacement is reported (Fig. 3a), together with the variation of the vertical forces (Fig. 3b). In this graph, variations over time are presented for clarity since they are the one considered in the experimental test; in the numerical model, they were adapted according to the different chosen load increments. The material properties, used as input in the model, were determined through standard laboratory tests and they are reported in

Table **1**. More detail about the mechanical characterization can be found in [11,12].

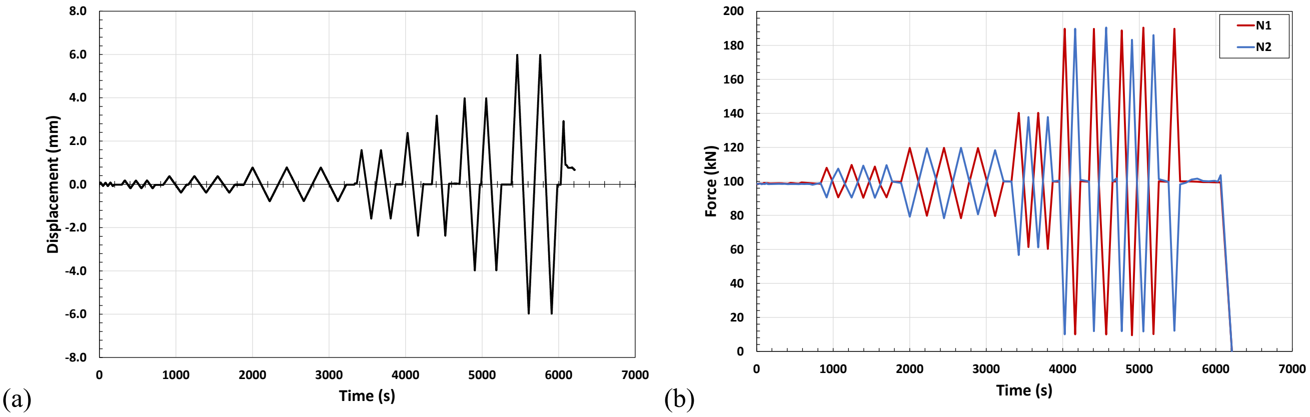

(a) (b)

Fig. 3. Testing procedure: (a) horizontal displacement *vs* time, (b) modulation of the vertical forces.

Table 1. Material properties.

Material	Property	Unit	Value
Concrete	Elastic modulus*	MPa	30000
	Poisson’s ratio*	-	0.2
Steel	Elastic modulus*	MPa	210000
	Poisson’s ratio*	-	0.3
Masonry (clay brick and lime-based mortar)	Elastic modulus	MPa	3900
	Poisson’s ratio	-	0.23
	Tensile strength	MPa	0.18
	Mode-I tensile fracture energy*	N/mm	0.02
	Compressive strength	MPa	4.5

*Not determined through experimental testing.

3.1 Predictive Numerical Model

Numerical simulations were carried out using the software Diana FEA 10.6. A Finite Element model (Fig. 4) of the innovative setup was realized by adopting quadratic plane stress elements for the testing sample (RC curb, RC foundation, and masonry panel). The horizontal steel beam at the top of the sample was modeled with flat shell and plate bending elements to reproduce the stiffeners as well. The RC foundation was clamped at the base and rollers support were modeled under the horizontal steel beam according to the real position of the rollers within the experimental setup.

Both RC elements and the top steel beam were considered linear elastic. Considering a macro-modelling approach [13], the masonry was modelled as a homogeneous and isotropic material. To reproduce a diagonal cracking failure mode of the masonry panel, the rotating total strain crack model [14] was considered, with exponential softening in tension, the Thorenfeldt model in compression [15] and the crack bandwidth defined by Rots [14]. Material properties used as input in the numerical simulation are reported in

Table **1**. Besides the ones obtained from experimental tests, the value of the first mode fracture energy was estimated considering analytical formulations available in literature [16].

To reproduce the rocking behavior as well, nonlinear interface elements (no tension material) were included between the masonry panel and the RC foundation (base), and between the RC curb and the steel beam (top). The normal and tangential elastic stiffness parameters were set as 10^6 N/mm^3 and 1000 N/mm^3, respectively.

Nonlinear phased analyses were carried out to reproduce the testing procedure described in Section 2.2. The regular Newton-Raphson method was used to solve the nonlinear problem.

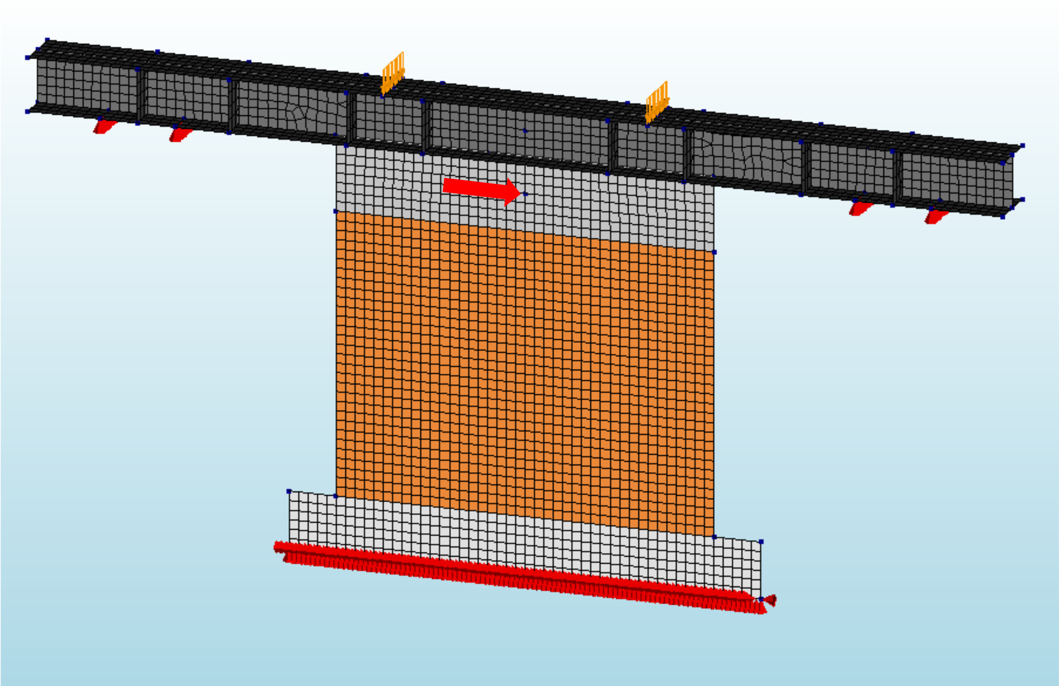

Fig. 4. Finite Element model.

In Fig. 5, the results in terms of in-plane principal stresses are reported with reference to the initial condition of the masonry panel, i.e., after the application of the vertical load (expected average vertical stress equal to 0.4 MPa), and with reference to the load cycle in which the first diagonal crack occurred, i.e., in correspondence with a positive displacement of 0.8 mm. After the first cracking, the failure progressed and further cracks formed, as can be seen in Fig. 6, where horizontal strains are presented for the last load cycles. In terms of vertical displacements (Fig. 7), it is possible to notice from Fig. 7b that limited displacements were registered at the top of the panel during the analysis, determining small rotations of the top cross section, as will be discussed in the following. The rocking failure was not activated, as confirmed by the negligible relative normal displacements registered along the interface elements at the top and at the bottom of the test sample.

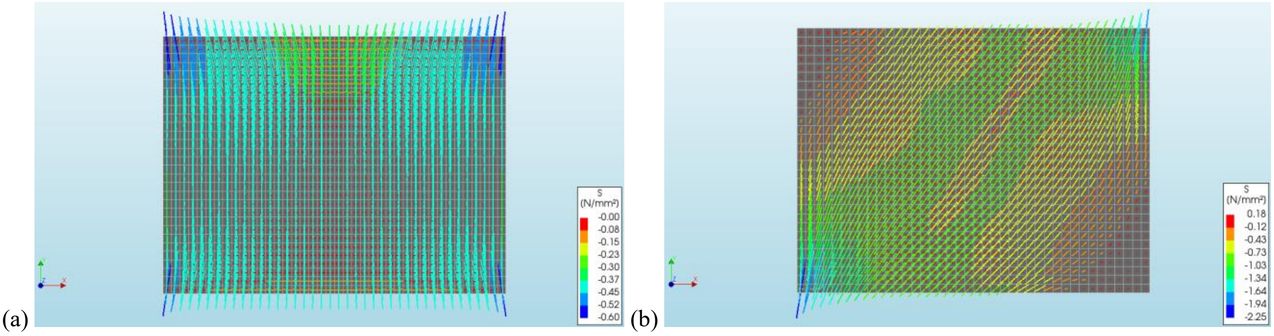

Fig. 5. In-plane principal stresses on the masonry panel: (a) application of the vertical load, (b) first cracking (load cycle at a horizontal displacement of 0.8 mm).

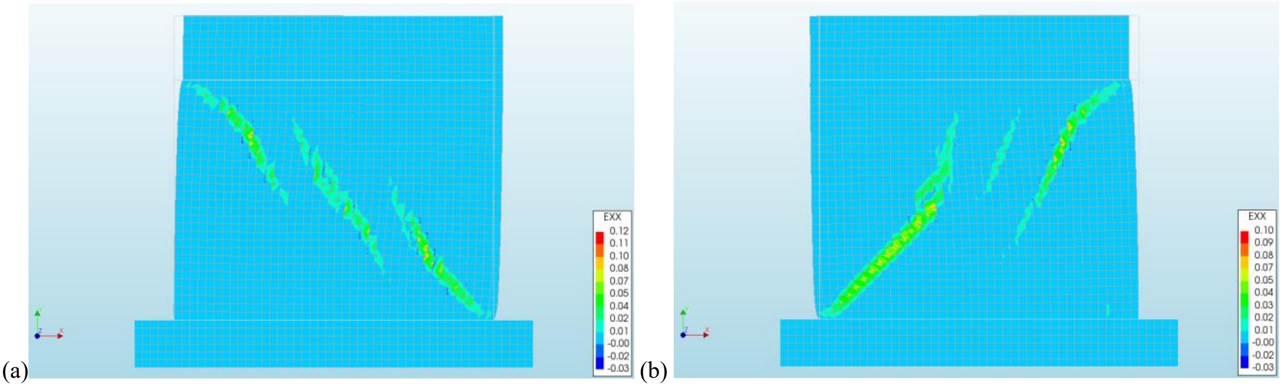

Fig. 6. Horizontal strains at the end of the simulation (horizontal displacement equal to 6 mm): (a) positive and (b) negative directions.

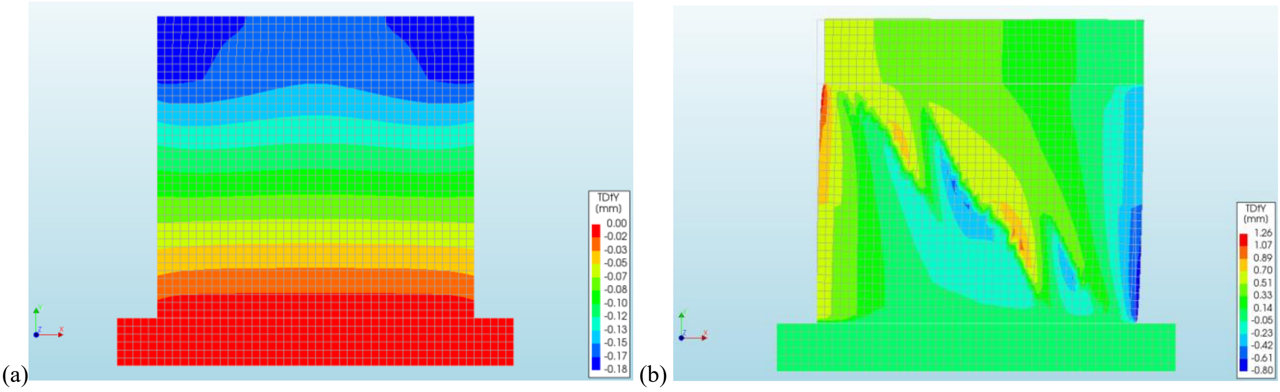

Fig. 7. Vertical displacements: (a) after the application of the vertical load, (b) load cycle at a horizontal displacement of 5 mm.

3.2 Experimental Test

The experimental test setup for the shear-compression test is presented in Fig. 8, corresponding to the description reported in Section 2.1. During the test, horizontal and vertical displacements were measured by means of Linear Variable Displacement Transducers (LVDTs), while diagonal displacements were monitored with linear potentiometers. In more detail, LVDTs were positioned to monitor the drift of the masonry panel and the relative displacements between the RC foundation, the masonry wall, the RC curb and the steel beam. The disposition of the instruments during the test is schematically reported in Fig. 9. On one side of the masonry panel (Fig. 9b), the Digital Image Correlation (DIC) technique was applied.

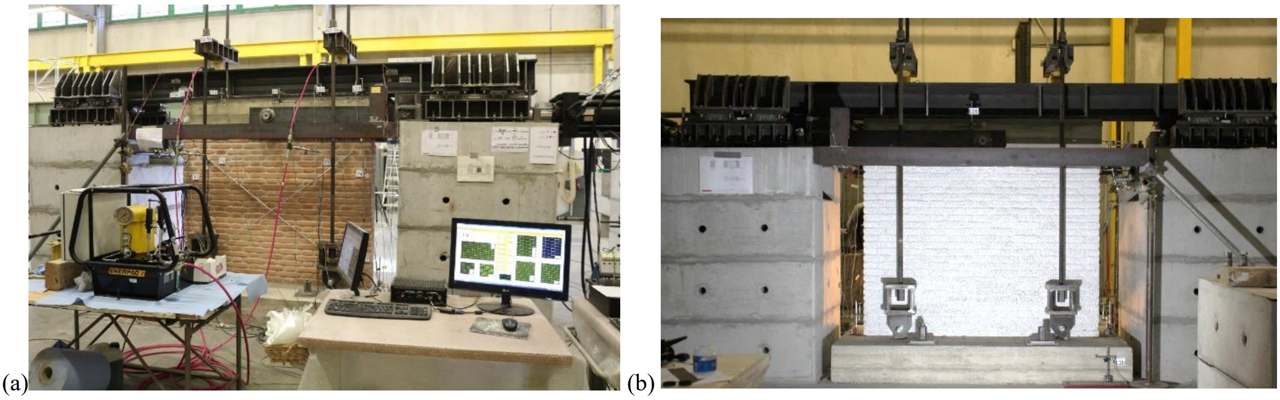

Fig. 8. Experimental setup of the shear-compression test.

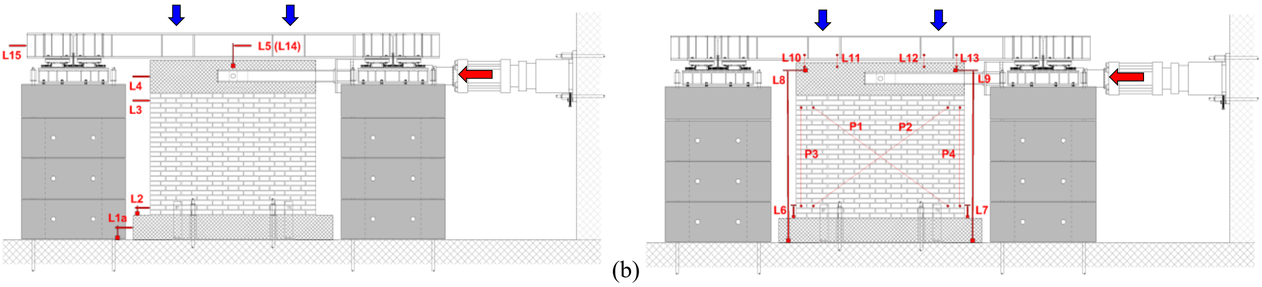

(a) (b)

Fig. 9. Experimental setup: (a) instruments to measure horizontal displacements, (b) instruments to measure vertical and diagonal displacements.

During the experimental test, the activation of a diagonal cracking failure mechanism was clearly detected, with the first inclined crack appeared in correspondence with a horizontal displacement approximately equal to 2 mm. The failure mode of the masonry panel is shown in Fig. 10. From the results reported in Fig. 11, it is worth noting that the base uplift was negligible in the first part of the test and the same applies for the vertical displacements measured by the potentiometers. Non-negligible displacement values were observed in the final part of the test due to the progressive damage of the panel. Similar observations can be made for the relative vertical displacements between the RC curb and the steel beam; thus, the detachment was limited. These outcomes confirm that the flexural behavior (rocking) of the panel was prevented, as well as a sliding shear behavior. Indeed, the horizontal relative displacements between the masonry panel and the RC elements and between the RC curb and the horizontal steel beam were negligible.

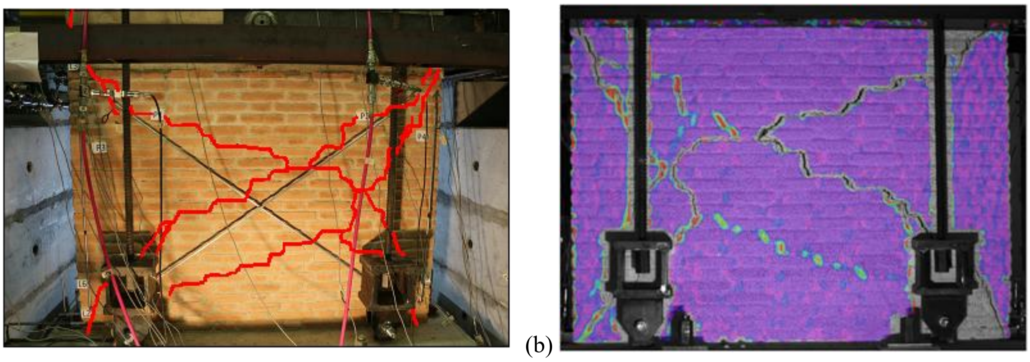

(a) (b)

Fig. 10. Failure mode of the masonry panel: (a) observed crack pattern, (b) horizontal strain map obtained with the DIC.

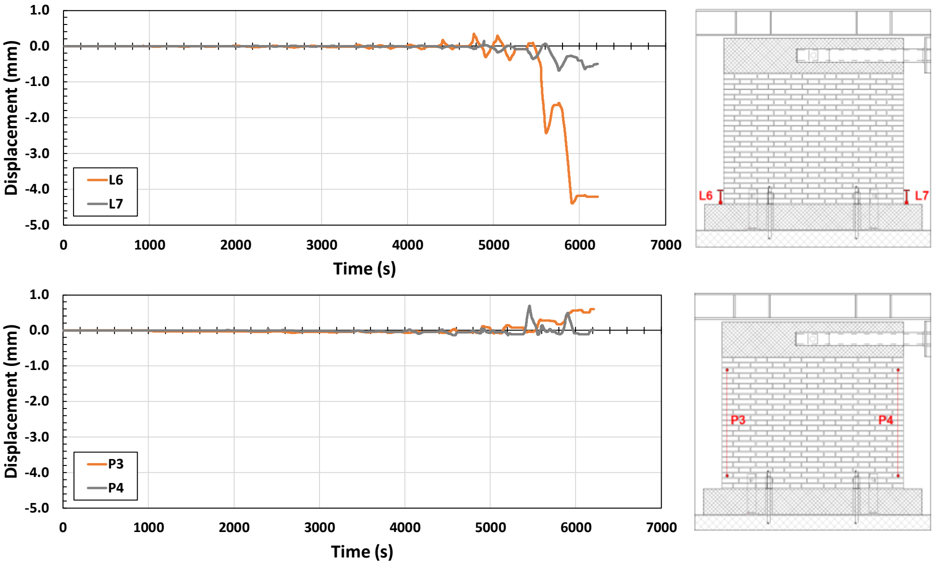

Fig. 11. Base uplift and vertical displacements.

3.3 Numerical vs Experimental Results

In this Section, a comparison between the main results obtained from the predictive numerical simulation and the experimental test is presented. First of all, it should be mentioned that, in both cases, a diagonal cracking failure mode was obtained, even if the first cracking developed in correspondence of two different values of the applied horizontal displacement. In terms of force *vs* displacement diagram (Fig. 12a), it can be observed that the numerical curve is characterized by a stiffer behavior, by a slightly higher maximum loads (in the positive and negative directions) and by a lower dissipative capacity. This can be related to the specific features of the total strain crack model, which was found to be not capable of properly reproducing the damage process occurring during shear failure.

In terms of force *vs* rotation (Fig. 12b), the experimental results were higher than the numerical ones for each load cycle. However, by comparing these values with different predictive models (Fig. 13), it was observed that the experimental behavior was in between the condition of a perfectly double fixed boundary condition, obtained imposing a very high stiffness to the horizontal beam, and the cantilever scheme, obtained by removing the horizontal steel beam from the model. A third comparison is also provided, in which the theoretical rotation of a cantilever beam, having the geometrical and mechanical properties of the masonry wall, was determined cycle by cycle, considering the secant stiffness derived from the experimental results.

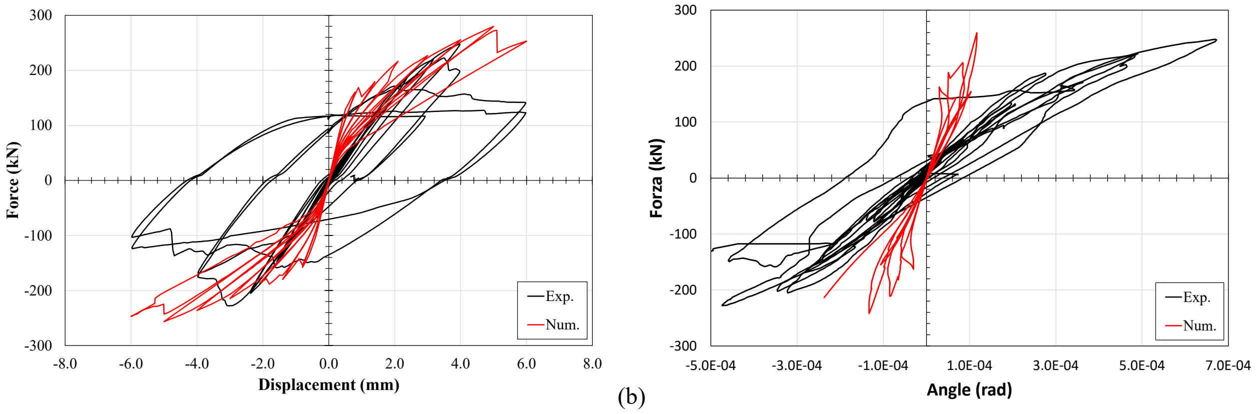

(a) (b)

Fig. 12. Experimental and numerical results comparison: (a) force *vs* displacement curve, (b) force *vs* rotation of the top cross section.

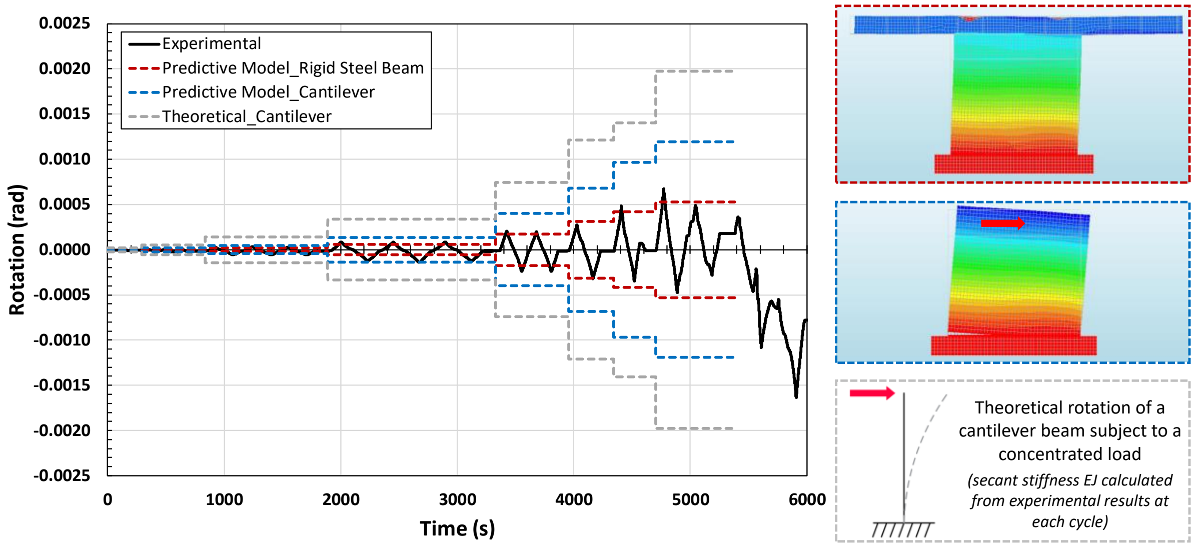

Fig. 13. Rotation of the top cross section: comparison between experimental results and predictive or theoretical models.

A comparison in terms of relative vertical displacements between the RC curb and the horizontal steel beam along the wall length is presented in Fig. 14, where positive values indicate a detachment. Very limited differences were noticed between experimental and numerical results for two drift values, confirming the observations previously made about the prevention of a rocking failure mechanism.

Finally, a check about the migration of the applied vertical force (N) on the vertical RC supports was carried out. In the numerical model, the force acting on the vertical RC supports during the analysis was estimated by considering the vertical reactions given by the roller restrains. In the experimental tests, the shear on the horizontal beam, equivalent to the amount of force migrating towards the RC supports, was derived by combining the deformations obtained in three different directions on the web of the beam, measured through three strain gauges, positioned on the web of the steel beam in the portions between the test sample and the rollers. A limited migration of the vertical force, corresponding to a vertical stress variation lower than 10%, was observed on both sides before the activation of the cracking process. This result was confirmed both experimentally and numerically.

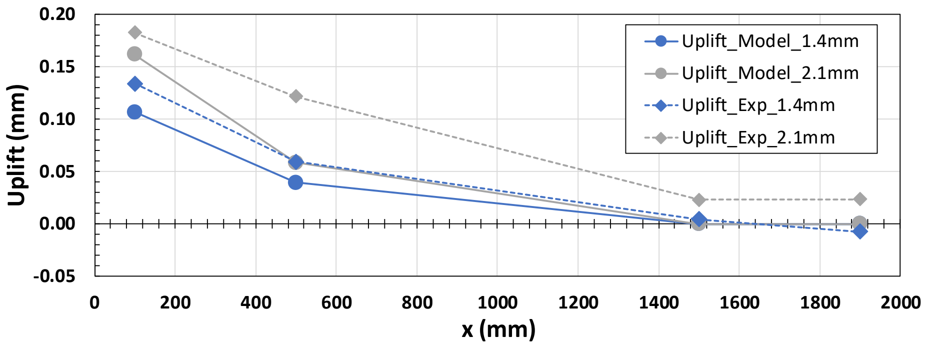

Fig. 14. Relative displacements between RC curb and horizontal steel beam for two horizontal displacement values.

4 Conclusions

In the present work, an innovative experimental setup for the execution of shear-compression tests on masonry panels was proposed. The system was designed to simulate a double fixed boundary condition, obtained by limiting the rotation of the top cross section thanks to the possibility of modulating the vertical load during the tests and to the presence of a horizontal rigid steel beam supported by rollers. Together with these aspects, the geometry of the test sample was chosen so to induce a diagonal cracking failure mode in presence of a vertical stress compatible with stress values typically acting on existing masonry walls.

Through a predictive nonlinear numerical simulation, it was confirmed the suitability of the setup in simulating the desired boundary condition and the shear failure mode, avoiding flexural failure (rocking) and sliding failure. These results were also confirmed by the outcomes of the first experimental test. In more detail, a similar cracking pattern, with diagonal cracks, was obtained in both cases and, even if differences were detected in terms of force *vs* displacement curves, a quite good agreement was obtained between the experimental and the numerical outcomes, especially considering the predictive nature of the numerical simulations.

Acknowledgements

The financial support of the Italian Department of Civil Protection (ReLUIS 2022-24 Grant – Innovative Materials) is gratefully acknowledged. The technical staff at CIRI Buildings & Construction is gratefully acknowledged for the collaboration during the preparation and execution of the tests.

References

1. Magenes, G., Calvi, M.: In-plane seismic response of brick masonry walls. Earthquake Engineering & Structural Dynamics 26, 1091-1112 (1997).
2. Calderini, C., Cattari, S., Lagomarsino, S.: In-plane strength of unreinforced masonry piers. Earthquake Engineering & Structural Dynamics 38, 243-267 (2009).
3. Ferretti, F., Ferracuti, B., Mazzotti, C., Savoia, M.: Destructive and minor destructive tests on masonry buildings: experimental results and comparison between shear failure criteria. Construction and Building Materials 199, 12-29 (2019).
4. Ongaretto, E., Pozza, L., Savoia, M.: Wood-based solutions to improve quality and safety against seismic events in conservation of historical buildings. International Journal for Quality Research 10(1), 17-46 (2016).
5. Scotta, R., Trutalli, D., Marchi, L., Pozza, L.: Seismic performance of URM buildings with in-plane nonstiffened and stiffened timber floors. Engineering Structures 167, 683-694 (2018).

6. van Vliet, M.R.A.: TNO report 2004-CI-R0171: Shear tests on masonry panels; Literature survey and proposal for experiments. TNO Building and Construction Research, The Netherlands (2004).
7. Wilding, B.V., Dolatshahi, K.M., Beyer, K.: Shear-compression tests of URM walls: Various setups and their influence on experimental results. Engineering Structures 156, 472-479 (2018).
8. Ganz, H.:Versuche an Mauerwerksscheiben unter Normalkraft und Querkraft, Bericht nr. 7502-4. Institut für Baustatik und Konstruktion ETH, Zurich (1984).
9. Woodward, K., Rankin, F.: Shear resistance of unreinforced hollow concrete block masonry walls. In: Proceedings of the 3rd North American Masonry Conference, Arlington, Texas (1985).
10. Epperson, G.S., Abrams, D.P.: Evaluating lateral strength of existing unreinforced brick piers in the laboratory. In: Proceedings of the 5th North American Masonry Conference, Urbana-Champaign, Illinois (1990).
11. Ferretti, F., Incerti, A., Mazzotti, C.: Experimental and Numerical Studies on the Shear-Sliding Behavior of Clay Brick Masonries. In: Proceedings of the 17th International Brick and Block Masonry Conference (IBMAC), Krakòw, Poland (2020).
12. Buratti, N., Cattari, S., Lignola, G., Meoni, A., Parisi, F., Ubertini, F., Virgulto, G.: DETECT-AGING blind prediction contest: a benchmark for structural health monitoring of masonry buildings. In: Proceedings of the ANIDIS Conference, Turin, Italy (2022).
13. Lourenço, P.B.: Computational strategies for masonry structures. PhD Thesis, Delft University of Technology, The Netherlands (1996).
14. Rots, J.G., Blaauwendraad, J.: Crack models for concrete: discrete or smeared? Fixed, multi-directional or rotating? HERON 34(1) (1989).
15. Thorenfeldt, E., Tomaszewicz, A., Jensen, J.J.: Mechanical properties of high-strength concrete and application in design. In: Proceedings of the Symposium Utilization of High-Strength Concrete, Tapir, Trondheim (1987).
16. Diana 10.6 User Manual, Ed. Denise Ferreira & Jonna Manie, DIANA FEA BV, Delft, The Netherlands (2022).